arXiv:hep-lat/9612004v1 5 Dec 1996

CCNY-HEP-96/7
hep-lat/9612004
May 1996

A Strong-Coupling Analysis of the Lattice CP^{N-1} Models in the Presence of a θ Term

Jan C. Plefka [1]

and

Stuart Samuel [2]

Department of Physics
City College of New York
New York, NY 10031, USA

Abstract

A θ term, which couples to topological charge, is added to the lattice CP^{N-1} model. The strong-coupling character expansion is developed. The series for the free energy and mass gap are respectively computed to tenth order and fourth order. Several features of the strong-coupling analysis emerge. One is the loss of superconfinement. Another is that in the intermediate coupling constant region, there are indications of a transition to a deconfining phase when θ is sufficiently large. The transition is like the one which has been observed in Monte Carlo simulations of a similar lattice CP^{N-1} action.

[1] E-mail address: plefka@scisun.sci.ccny.cuny.edu

[2] E-mail address: samuel@scisun.sci.ccny.cuny.edu

I. Introduction

One of the unresolved puzzles of the standard model is the strong CP problem. The problem emerged after the discovery of instantons in four-dimensional Yang-Mills theories [1]. Instantons represent barrier penetration processes between different classical n-vacua. The "true" quantum vacua are believed to be linear combinations of n-vacua weighted by a phase $\exp(in\theta)$ [2, 3]. Alternatively, one can add $\theta \int d^4x\nu(x)$, where $\nu(x) = g^2 F^a \tilde{F}^a(x)/(32\pi^2)$, to the action lagrangian. Here, $\int d^4x\nu(x) = Q$ is the topological charge. It is one (minus one) for an instanton (anti-instanton). The action term $\theta \int d^4x\nu(x)$ breaks parity, time-reversal invariance and CP symmetry. Although the θ-term is a total derivative so that it does not contribute in perturbative Feynman diagrams, instantons and topological quantum fluctuations contribute to it. Such topological fluctuations are known to exist because they contribute significantly to the η' mass [4]–[8]. Lattice simulations have computed these topological fluctuations and yield results of the right magnitude to explain $m_{\eta'}$ [9]–[13].

When quarks are included, phases in the quark mass matrix $\mathcal{M}$ contribute to CP violation also. Using a $U(1)$ axial rotation, a common phase in $\mathcal{M}$ can be shifted to the θ-term due to the axial anomaly [14, 15]. The physical effective theta parameter θ_{eff} is $\theta_{eff} = \theta + ArgDet\mathcal{M}$. A non-zero value of θ_{eff} contributes, among things, to the electric dipole moment of the neutron. Requiring compatibility with experiment leads to $\theta_{eff} \lesssim 10^{-9}$ [16, 17]. The difficulty in understanding how θ_{eff} can naturally be so small constitutes the strong CP problem.

Various solutions to the strong CP problem have been proposed [18, 19, 20]. Perhaps the most theoretically attractive suggestion is the Peccei-Quinn mechanism [21]. It predicts the existence of an axion [22, 23]. Such an axion has not been seen in accelerator experiments. A modification of the mechanism leads to an invisible axion [24]–[27]. Astrophysical considerations and accelerator experiments have left open a somewhat narrow mass window for the invisible axion [28].

Another possible solution is that the current-algebra mass of the up quark is zero [29, 30, 31]. Various analyses suggest that the up-quark mass is non-zero and equal to about 5 MeV [32, 33]. However, the up-quark mass has been the subject of much

debate and some theorists feel that a zero value is not ruled out [34].

The Peccei-Quinn mechanism involves a relaxation field which allows θ_{eff} to be rotated away. This field is the axion. In ref. [35], a $2+1$ dimensional model was considered in which the Yang-Mills sector generated its own relaxation field. This led to a natural solution to the strong CP problem within the pure Yang-Mills sector. Criteria were established to determine when such a natural relaxation mechanism arises [35]. Unfortunately, it has not been possible to determine whether or not these criteria are satisfied for four-dimensional Yang-Mills theories.

The strong CP problem in a pure Yang-Mills theory involves vacuum physics. Vacuum physics is governed by the long-distance behavior of a theory. The long-distance behavior of non-abelian gauge theories involves non-perturbative and strong-coupling effects. Since this regime is not so theoretically well understood, there is the possibility that some subtle mechanism exists which resolves the strong CP problem naturally.

Given the complexity of the strong CP problem, it is useful to consider simpler systems. One class of such systems is the two-dimensional CP^{N-1} models. These models are asymptotically free and have instantons for all $N \geq 2$. In addition, a θ-term can be added to the action. The analysis in the large N limit leads to considerable insight into their physics [36, 37]. The θ dependence is expected to be a $1/N$ effect – this contrasts the exponentially suppressed behavior $\exp(-cN)$ expected from an instanton analysis [37]. In the leading order $1/N$ result, the CP^{N-1} models consist of N free particles and N free antiparticles, and there is no θ dependence. When the first $1/N$ correction is taken into account, quantum fluctuations produce a dynamically generated $U(1)$ gauge field which, in turn, generates a constant force between particles and antiparticles, thereby leading to confinement. The free energy $\mathcal{F}$ per unit volume behaves as $c\theta^2/N$, where c is a constant. It is expected that the confining force becomes stronger and stronger as higher-order $1/N$ corrections are included since the CP^{N-1} models exhibit superconfinement [38]. In a theory with superconfinement, the confining force is so strong that an antiparticle must be positioned on a particle. Not only is there confinement at asymptotic distances but there is local confinement as well – particles and antiparticles in a bound state cannot

be separated at all. The dramatic changes in behavior in going from leading order to next-to-leading order are indicative of the singular nature of the $1/N$ expansion in the CP^{N-1} models. The singular nature is also reflected in the fact that strong coupling and $1/N$ expansions do not commute [38].

G. Schierholz and co-workers have performed Monte Carlo simulations on the two-dimensional CP^3 model with a θ term [39]. A priori surprising results have emerged. For fixed inverse coupling β, a phase transition occurs as a function of θ. Letting θ_c denote the critical value, the free energy per unit volume is well represented by

$$\mathcal{F} = \begin{cases} a\,(\beta)\,\theta^2 & \theta \leq \theta_c \\ c\,(\beta) & \theta \geq \theta_c \end{cases} \quad . \tag{1.1}$$

In other words, for $\theta \geq \theta_c$, the free energy has no dependence on θ. In two dimensions, this implies that the string tension vanishes for $\theta \geq \theta_c$ so that confinement is lost. Furthermore, θ_c appears to go to zero as the coupling g goes to zero (or β goes to infinity). The behavior of $\mathcal{F}$ for $\theta \leq \theta_c$ is compatible with the next-to-leading order $1/N$ result. This is not the case for $\theta > \theta_c$. Since additional $1/N$ corrections have not been computed, it is unclear whether there is a discrepancy.

The two-dimensional Schwinger model has a cusp in the free energy at $\theta = \pi$, signaling the spontaneous breaking of CP invariance [40]. A similar phenomenon is expected in the CP^{N-1} models. In fact, at infinite coupling, $\beta = 0$, the lattice CP^{N-1} models do undergo spontaneous CP breaking at $\theta = \pi$ [41]. Hence, a phase transition with $\theta_c = \pi$ is not unexpected. The surprising feature of the CP^3 model is the dependence of θ_c on β [39]. It suggests that to obtain a confining theory from the continuum limit of a lattice CP^{N-1} model, one must take θ to zero. Thus it appears that continuum confining CP^{N-1} models must have $\theta = 0$. If the analog statement were true for a four-dimensional Yang-Mills theory, then the strong CP problem would be solved.

An analysis [42] of the free energy of the four-dimensional $SU(2)$ Yang-Mills theory indicates that the free energy behaves as in equation (1.1). In contrast to two-dimensional systems, however, a constant $\mathcal{F}$ behavior for $\theta \geq \theta_c$ does not necessarily indicate a loss of confinement. Nonetheless, if θ must be selected to be less than θ_c for certain as-of-yet-unknown physical reasons and θ_c goes to zero as $\beta \to \infty$, then the

strong CP problem would be solved. Up to now, simulations of the four-dimensional $SU(2)$ gauge theory have been done at only one value of β, so that it is not known whether θ_c goes to zero as $\beta \to \infty$.

Since the strong CP problem is related to long-distance physics and since long distances are equivalent to strong couplings in an asymptotically free theory, it is of interest to perform lattice strong-coupling expansions. As far as we know, only one strong-coupling expansion has been performed in the presence of a θ term. The zeroth order and order β^2 terms for the free energy and mass gap were obtained in ref. [41]. Strong-coupling series are best organized in character expansions. Character expansions were introduced in ref. [43] for lattice gauge theories. They were obtained for matrix-model spin systems and for the large N limit in [44]. Finally, the adaptation of such methods to vector-like spin systems, including the CP^{N-1} models, was achieved in [45, 46]. As far as we know, the techniques for performing character expansions in the presence of a θ term have not yet been developed. One of the purposes of the current work is to fill this need. Another purpose is to gain insight from such analytic strong-coupling computations into the physics associated with θ. Strong-coupling analysis is often one of the best ways to gain an understanding into the non-perturbative long-distance behavior of asymptotically free theories. It was by these means, for example, that K. Wilson demonstrated that non-abelian gauge theories have the potential to confine quarks in four dimensions [47].

II. Methodology

The action for the continuum CP^{N-1} model is

$$S = \beta N \int d^d x \left(\partial_\mu z_i^* \partial^\mu z^i + \left(z_i^* \partial_\mu z^i \right) \left(z_j^* \partial^\mu z^j \right) \right) \quad , \tag{2.1}$$

where $z(x)$ is an N-component complex field satisfying $z_i^* z^i(x) = 1$. Eq. (2.1) possesses the local symmetry $z(x) \to \exp(i\alpha(x)) z(x)$. Hence, the local gauge-invariant degrees of freedom at a point x live on the manifold CP^{N-1}. Using an auxiliary field $A_\mu(x)$, the action in Eq. (2.1) can be written as

$$S = \beta N \int d^d x \left(\partial_\mu - i A_\mu \right) z_i^* \ \left(\partial^\mu + i A^\mu \right) z^i \quad . \tag{2.2}$$

Quantum fluctuations turn $A_\mu(x)$ into a propagating field. It becomes the $U(1)$ field mentioned in the Introduction and confines the charged $+1$ particles z_i^* to the charged -1 particles z_i.

There are always many equally satisfactory ways to latticize a continuum action. For the CP^{N-1} models, two lattice actions naturally arise – they correspond to the naive discretization of Eqs. (2.1) and (2.2). A lattice version of (2.1) is

$$S = \beta N \sum_{x,\Delta} z^*_{x+\Delta} \cdot z_x \; z^*_x \cdot z_{x+\Delta} \quad , \tag{2.3}$$

while a lattice version of (2.2) is

$$S = \beta N \sum_{x,\Delta} \left(z^*_x \cdot z_{x+\Delta} \exp\left(iA_{x,x+\Delta}\right) + z_x \cdot z^*_{x+\Delta} \exp\left(-iA_{x,x+\Delta}\right) \right) \quad . \tag{2.4}$$

In Eqs. (2.3) and (2.4), the sum over Δ involves the d positively-directed nearest neighbors to x, so that Δ takes on the values e_1, e_2,..., e_d, where e_i is a unit vector in the ith direction. In what follows, we restrict to the case of two dimensions so that $d = 2$.

For the action in (2.3), a θ term is defined as follows [48]. Associate a $U(1)$ field $U\left(x, x+\Delta\right)$ with each link via $U\left(x, x+\Delta\right) = z^*_x(x) \cdot z_{x+\Delta} / |z^*_x(x) \cdot z_{x+\Delta}|$. Let U_p be the product of the $U\left(x, x+\Delta\right)$ around a plaquette. Define the local topological density ν_p via $\nu_p \equiv log\left(U_p\right)/(2\pi)$. The branch of the logarithm is taken to be between $-\pi$ and π. The total topological charge Q is $Q = \sum_p \nu_p$. The θ term to be added to the action is $i\theta Q$, that is,

$$S_{\theta \text{ term}} = \frac{i\theta}{2\pi} \sum_p log\left(U_p\right) \quad . \tag{2.5}$$

The θ term is a complicated function of the $z(x)$.

For the auxiliary gauge field formulation in Eq. (2.2), a θ term can be defined by setting the link variable $U\left(x, x+\Delta\right)$ to be $\exp\left(iA_{x,x+\Delta}\right)$, letting U_p be the product of the link variables around a plaquette and using Eq. (2.5).

At strong coupling, field configurations fluctuate considerably and might lead to bad behavior in Eq. (2.5). However, fluctuations are not so severe as to render Eq. (2.5) so singular that strong-coupling computations cannot be performed. In fact,

ref. [41] found no computational difficulties in leading order. Likewise, no difficulties arose in the higher order calculations of the current work.

Boundary conditions determine whether Q is quantized. The analysis can be performed in a model-independent way. Since one is dealing with gauge-invariant functions of a compact $U(1)$ field, one can transform to a set of independent gauge-invariant degrees of freedom. In two-dimensions with open boundary conditions, the plaquette variables U_p are such a set. Writing $U_p = \exp(if_{ij})$ with $-\pi < f_{ij} \leq \pi$, Figure 1 shows a configuration of $U(1)$ fields which produces the most general configuration of the U_p. In this figure, most link variables equal 1. A Wilson loop which runs around the boundary of the lattice has the value $\exp(i\sum_{ij} f_{ij})$. Since this factor is not necessary 1, Q need not be an integer.

With periodic boundary conditions, the most general configuration is that of Figure 1 with $\exp(i\sum_{ij} f_{ij}) = 1$ and for which all horizontal links are multiplied by $\exp(i\alpha_1)$ and all vertical links are multiplied by $\exp(i\alpha_2)$. These constant phases do not change the value of U_p but allow the Polyakov lines at the lower-most and left-most sides of Figure 1 to be non-zero. Since the condition $\exp(i\sum_{ij} f_{ij}) = 1$ implies that $\sum_{ij} f_{ij} = 2\pi Q$, Q is integer. The constraint can be handled by inserting $\sum_Q \delta\left(\sum_{ij} f_{ij}/(2\pi) - Q\right)$ into the functional integral. This makes the dependence on θ periodic since the following combination arises in the functional integral

$$\exp\left(i\frac{\theta}{2\pi}\sum_{ij} f_{ij}\right)\sum_Q \delta\left(\sum_{ij} f_{ij}/(2\pi) - Q\right) = \sum_m \exp\left(i\frac{\theta+2\pi m}{2\pi}\sum_{ij} f_{ij}\right) \quad . \tag{2.6}$$

Here, the resummation formula $\sum_Q \delta\left(\sum_{ij} f_{ij}/(2\pi) - Q\right) = \sum_m \exp\left(im\sum_{ij} f_{ij}\right)$ has been used.

For the action in Eq. (2.4), the change from link variables to plaquette variables U_p can be explicitly performed with unit Jacobian. At $\beta = 0$, the integrand for the partition function $Z(\beta = 0)$ is Eq. (2.6), where the measure is $\prod_{ij}\int_{-\pi}^{\pi} df_{ij}/(2\pi)$:

$$Z(\beta)|_{\beta=0} = \sum_m \left[\frac{2}{\theta+2\pi m}\sin\left(\frac{\theta+2\pi m}{2}\right)\right]^V \quad , \tag{2.7}$$

where V, the number of sites of the lattice, is the volume of the system. The free

energy $\mathcal{F}$ per unit volume, defined by $\mathcal{F} = -\lim_{V\to\infty}(\log Z)/V$, is

$$\mathcal{F} = -\log\left(\frac{2}{\theta}\sin\left(\frac{\theta}{2}\right)\right) \quad , \quad \text{for } -\pi < \theta \leq \pi \quad , \tag{2.8}$$

and $\mathcal{F}$ is determined by periodicity in θ when θ is outside the range from $-\pi$ to π. Eq. (2.8) is the result obtained in ref. [41]. In what follows, we use periodic boundary conditions so that all quantities are periodic functions of θ with period 2π. Formulas below are written for the case $-\pi < \theta \leq \pi$.

To develop strong-coupling character expansions, we have found it calculationally more convenient to use the auxiliary gauge field formulation. Hence, throughout the rest of this work, we use the action which is the sum of Eqs. (2.4) and (2.5). The expansion procedure is similar to the one discussed in ref. [38]: One performs a group-theoretic-like Fourier decomposition of the action associated with each link. However, because of the θ term, one cannot immediately perform the integrations over the auxiliary gauge fields. One writes

$$\exp\beta N\left[z_x^*\cdot z_{x+\Delta}\exp\left(iA_{x,x+\Delta}\right) + z_x\cdot z_{x+\Delta}^*\exp\left(-iA_{x,x+\Delta}\right)\right] =$$

$$Z_0(\beta)\sum_{m,n} d_{(m;n)}\,\exp\left[i(n-m)A_{x,x+\Delta}\right] z_{(m;n)}(\beta)\, f_{(m;n)}\left(z_x, z_{x+\Delta}\right) \quad , \tag{2.9}$$

where $Z_0(\beta)$ is a normalization factor and where the sum is over non-negative integers m and n. Character-like "representations" r are governed by the pair $(m;n)$: $r = (m;n)$. Here, d_r, z_r and f_r are respectively character-like dimensions, expansion coefficients and representations for the $U(N)$ vector models [38]. See Appendix A for explicit formulas for low orders.

With the appropriate normalization of the $f_{(r)}$, one has

$$\int dv\, f_r(w,v)\, f_{r'}^*(w',v) = \frac{1}{d_r}\,\delta_{r\,r'}\, f_r(w,w') \quad , \tag{2.10}$$

and

$$f_r(w,w) = d_r \quad . \tag{2.11}$$

The calculational procedure is to expand the action of each link as in Eq. (2.9) and then perform the integrations over the $z(x)$ using Eq. (2.10). Lastly, one does the integration over the auxiliary gauge fields. Such integrations involve Wilson loops.

Using Stoke's theorem, such Wilson loops can be written as products over plaquettes of plaquette variables to various powers. The result

$$\frac{\int dU_p \exp\left[\frac{i\theta}{2\pi} log\left(U_p\right)\right] {U_p}^n}{\int dU_p \exp\left[\frac{i\theta}{2\pi} log\left(U_p\right)\right]} = (-1)^n \left(\frac{\theta}{\theta + 2\pi n}\right) \tag{2.12}$$

is useful.

III. Results

It is straightforward to compute the partition function using the character-like expansion in Eq. (2.9) and the above-mentioned procedure. Exponentiation of volume factors naturally occurs so that $Z = \exp(-V\mathcal{F})$ where $\mathcal{F}$ is the free energy per unit volume. We have computed $\mathcal{F}$ to tenth order, which is four more terms than in ref. [41]. When expanded in β up to order β^2, our results agree with those of ref. [41]. The fourth, sixth, eighth and tenth orders provide new information about the CP^{N-1} models in the presence of a θ term. Because the result for $\mathcal{F}$ is rather lengthy, we have relegated it to Appendix B. See Eq. (B.1).

An analysis of the strong-coupling expansion leads to some immediate physical results. The first is the loss of superconfinement when $\theta \neq 0$. When $\theta \neq 0$, strong-coupling diagrams appear in fourth and higher order terms in which a positively charged loop does not have to be directly on top of a negatively charged loop. Local charge liberation occurs. Charges are no longer superconfined. Instead they are bound together by ordinary confinement. Thus, the confining force is weakened. Furthermore, charged loops oriented counterclockwise arise with probabilities which are different from loops oriented clockwise. This is expected and is an indication of the explicit CP violation generated by a θ term when $\theta \neq 0$ or $\theta \neq \pi$.

For β small, higher order terms do not significantly change the result in Eq. (2.8): $\mathcal{F}$ increases as $|\theta|$ increases and its graph is concave upward. As β becomes larger, $\mathcal{F}$ is lowered particularly for larger values of θ. Then, for sufficiently large β a maximum in $\mathcal{F}$ arises at θ near $\pm\pi$. Figure 2a illustrates this for the $N = 4$ case. Other values of N are qualitatively similar. As β is further increased, the maximum in $\mathcal{F}$ occurs at smaller values of θ. See Figure 2b which plots $\mathcal{F}$ versus θ when $\beta = 0.7$. For the

$N = 4$ case, the maximum eventually reaches $\theta = 0$ for $\beta \approx 0.90$. However, at these moderate values of β, higher order terms might be important.

In two dimensions the string tension $\sigma(e, \theta, \beta)$ between a charge e and a charge $-e$ can be obtained from the free energy via the standard formula $\sigma(e, \theta, \beta) = \mathcal{F}(\theta + 2\pi e, \beta) - \mathcal{F}(\theta, \beta)$.[49] Hence, the value of θ at which the free energy stops increasing and begins to decrease marks the point where confinement is lost for infinitesimal charges. Using our results for $\mathcal{F}$, a phase diagram can be constructed. It is shown in Figure 3 for the CP^3 model. The reader should be forewarned that this phase diagram is obtained under the assumption that strong coupling results can be extrapolated to moderate values of β. The dotted line in Figure 3 indicates where CP invariance spontaneously breaks. This line bifurcates at around $\beta = 0.56$. For β larger than 0.56 there are two phases as a function of θ. The region labeled "infinitesimal confinement loss" is where charges of very small magnitude no longer experience a confining force. The phase diagram of Figure 3, which is obtained by analytic methods, is qualitatively similar to the diagram of refs. [39], obtained from Monte Carlo simulations of the adjoint form of the CP^3 action in Eq. (2.3). We have also taken our tenth order series, expanded it in β, and obtained Padé approximates to try to increase the range of validity of our strong-coupling results. For the diagonal approximate, the β at which infinitesimal confinement loss first takes place is shifted to larger values. Even for β as large as 2.0, there is confinement for θ small. Hence, the phase diagram using the diagonal Padé approximate looks as in Figure 3 but with the lines separating the regions "full confinement" from "infinitesimal confinement loss" shifted to the right.

The mass gap m can be extracted from the two-point function:

$$\sum_x \langle z(0,0) \cdot z^*(x, L)\, z^*(0,0) \cdot z(x, L) \rangle \sim \exp(-mL) \tag{3.1}$$

Summing over x to project onto zero momentum makes it easier to compute m. The strong-coupling series for m at $\theta = 0$ has been obtained to tenth order in ref. [46]. The computation for $\theta \neq 0$ is considerably more complicated in that sets of graphs must be summed. Here, we compute m to order four when a θ term is present. This is one more order than the β expansion computation in ref. [41]. Our results agree with [46] and [41] for those terms which are in common. The computation of m is

lengthy and is relegated to Appendix B. See Eq. (B.2).

The second order θ-dependent term lowers the value of m. This is physically expected. The loss of superconfinement means that the charges can move more freely within the bound state, thereby lowering their constituent mass. However, the fourth order θ-dependent term counteracts the effect and tends to increase the value of m particularly for large θ. In Figure 4, we plot m versus β for various fixed values of θ. For sufficiently small β, m is lowered when θ is non-zero, but the effect is small and not too visible for the scales used in Figure 4. The curves for $\theta \leq 1.0$ are almost identical to the case $\theta = 0$ and are displayed as one curve. For $\theta > 1.0$, fourth order contributions increase m significantly at moderate values of β, however, at such β values, higher order terms can be important.

For sufficient large β, refs. [39] has observed a phase transition as θ is increased. A priori such a transition could be due to the vanishing of m. Our computation of m suggests that this is not the case and supports the conclusion that the transition is due to the loss of confinement. If confinement is lost, one expects on physical grounds that $m = 2m_0 > 0$ where m_0 is the mass of a free charged particle.

IV. Conclusions

In this work, we have developed and performed the first character expansions for a lattice model with a θ term. The purpose was to gain insight into the strong-coupling behavior of the physics associated with a topological term.

We found the following physical effects. The superconfinement property of the CP^{N-1} is lost for $\theta \neq 0$. When $\theta \neq 0$, superconfinement liberation occurs. A bound state still persists but is tied together by ordinary confining forces. The weakening of the binding in the bound state is reflected by the lowering of its mass at small β.

In Monte Carlo simulations, refs. [39] observed a phase transition when θ was increased. It was argued that this transition was associated with the loss of confinement. Our analytic computations, although not conclusive and performed with a different lattice version of the CP^{N-1} model, support this conclusion. Furthermore, the mass of the bound state does not appear to vanish at the deconfinement point.

The main motivation for our work is to gain insight into the strong CP problem. Our analytic computations support the conclusion of refs. [39] that the analog of

the strong CP problem is naturally resolved in the CP^{N-1} models. It was argued that, as $\beta \to 0$, θ must be adjusted to 0 as the continuum limit is taken in order to have a confining theory with bound states. Our analytic computations support this statement. Assuming that higher-order corrections do not invalidate results, the strong coupling computations show that θ must be decreased as β is increased to remain in the confining phase, but they are unable to say whether θ must be taken to zero as $\beta \to \infty$.

The conclusion concerning the strong CP problem appears rather specific to two dimensions. In two dimensions in the continuum, a θ term in the action produces an immediately physical effect – it introduces charges at spatial infinity which create a constant background electric field. This has a direct effect on a bound state. In four-dimensional gauge theories, a θ term affects physics more indirectly: If a theory possesses monopoles, then such monopoles acquire an electric charge proportional to θ [50]. In Monte Carlo simulations at a particular value of the coupling, ref. [42] has shown that the $SU(2)$ four-dimensional Yang-Mills theory has a dependence on θ similar to that of the CP^{N-1} models. In particular, a phase transition occurs at a certain value of θ. Given the difference between two and four dimensions, it is not probable that this transition is related to deconfinement. It is thus quite important to determine the physics associated with the transition to decide whether θ must be tuned to zero as the continuum limit is taken.

Acknowledgments

S. Samuel thanks Columbia University for hospitality and support. This work was supported in part by the Humboldt Foundation under a Lynen-Fellowship and by the National Science Foundation under the grant (PHY-9420615).

Appendix A: Characterlike Expansion Quantities

The leading order character-like representations f_r used in our computation are

$$\begin{aligned} f_{(0;0)}(v,w) &= 1 \ , \qquad\qquad f_{(1;0)}(v,w) = \sqrt{N}\, v \cdot w \ , \\ f_{(2;0)}(v,w) &= \sqrt{\frac{N(N+1)}{2}}\, (v^* \cdot w)^2 \ , \end{aligned}$$

$$
\begin{aligned}
f_{(1;1)}(v,w) &= N\sqrt{\frac{N+1}{N-1}}\Big[v^*\cdot w\, v\cdot w^* - \frac{1}{N}\Big]\ , \\
f_{(2;1)}(v,w) &= (N+1)\sqrt{\frac{N(N+2)}{2(N-1)}}\Big[v^*\cdot w\,(v\cdot w^*)^2 - \frac{2}{N+1}v\cdot w^*\Big]\ , \\
f^*_{(m;l)}(v,w) &\equiv f_{(l;m)}(v,w) \equiv f_{(m;l)}(w,v) \quad ,
\end{aligned}
\tag{A.1}
$$

and the corresponding dimensions d_r are

$$
\begin{aligned}
d_{(0;0)} &= 1\ , \qquad d_{(1;0)} = \sqrt{N}\ , \qquad d_{(2;0)} = \sqrt{\frac{N(N+1)}{2}}\ , \\
d_{(1;1)} &= \sqrt{N^2-1}\ , \qquad d_{(2;1)} = \sqrt{\frac{N(N-1)(N+2)}{2}}\ , \\
d_{(l;m)} &= d_{(m;l)} \quad .
\end{aligned}
\tag{A.2}
$$

These formulas can be derived with the help of the integral

$$
\int dv\, v_{i_1} v_{i_2}\ldots v_{i_m}\, v^*_{j_1} v^*_{j_2}\ldots v^*_{j_m} = \frac{(N-1)!}{(N-1+m)!}\sum_{\sigma\in S_m}\delta^{i_1}_{j_{\sigma(1)}}\delta^{i_2}_{j_{\sigma(2)}}\ldots\delta^{i_m}_{j_{\sigma(m)}}\ , \tag{A.3}
$$

where the sum is to be taken over all permutations of the j indices. In Eq. (A.3) and throughout this appendix we are using the following normalized notation for vector integrals

$$
\int dv\,(\ldots) = \frac{\int dv\,\delta(v^*\cdot v-1)\,(\ldots)}{\int dv\,\delta(v^*\cdot v-1)} \quad . \tag{A.4}
$$

The expansion coefficients $z_r(\beta)$ may be computed by inverting eq. (2.9) using eq. (2.10):

$$
z_{(l;m)}(\beta) = \frac{1}{d_{(l;m)}\,Z_0(\beta)}\int dv f_{(l;m)}(v,w)\,\exp[N\,\beta\,(v\cdot w^* + v^*\cdot w)] \quad . \tag{A.5}
$$

The $z_{(l;m)}(\beta)$ are actually independent of w and are of order $l+m$, i.e. $z_{(l;m)} = O(\beta^{l+m})$.

The factor $Z_0(\beta)$ normalizes $z_{(0;0)}$ to 1 and can be explicitly computed

$$
Z_0(\beta) = \frac{(N-1)!\,I_{N-1}(2\,\beta\,N)}{(\beta\,N)^{N-1}} \quad , \tag{A.6}
$$

where $I_n(x)$ is the Bessel function $I_n(x) = \int_{-\pi}^{\pi} d\theta/(2\pi)\,\exp[in\theta + x\cos\theta]$.

The $z_{(l;m)}(\beta)$ can also be explicitly computed and read

$$
z_{(0,0)} = 1\ ,
$$

$$
\begin{aligned}
z_{(1;0)} &= \frac{I_N(2\,\beta\,N)}{I_{N-1}(2\,\beta\,N)} \\
&= \beta - \frac{N}{N+1}\beta^3 + \frac{2\,N^2}{(N+1)(N+2)}\beta^5 \\
&\quad -\frac{\beta^7 N^3\,(5N+6)}{(N+1)^2\,(N+2)\,(N+3)} + \frac{2\beta^9 N^4\,(7N+12)}{(N+1)^2\,(N+2)\,(N+3)\,(N+4)} \\
&\quad -\frac{2\beta^{11} N^5\,(21N^3+118N^2+214N+120)}{(N+1)^3(N+2)^2\,(N+3)\,(N+4)\,(N+5)} + \dots\ , \\
z_{(2;0)} &= z_{(1;1)} = 1 - \frac{1}{\beta}\ z_{(1;0)}\ , \\
z_{(2;1)} &= -\frac{N+1}{\beta\,N} + \Big(1 + \frac{N+1}{\beta^2\,N}\Big)\ z_{(1;1)} \quad .
\end{aligned}
\tag{A.7}
$$

Here, we have displayed $z_{(1;0)}$ to order eleven. From this expansion, one can construct the ordinary β expansions of the free energy and mass gap.

After the expansion of each link as in eq. (2.9), one has to perform the integral over the vectors and the link angles. For the vectors it is convenient to make use of the relations

$$
\begin{aligned}
f_{(1;0)}\,f_{(1;0)} &= \sqrt{\frac{2N}{(N+1)}}\,f_{(2;0)}\ , \\
f_{(1;0)}\,f_{(0;1)} &= \sqrt{\frac{N-1}{N+1}}\,f_{(1;1)} + f_{(0;0)}\ , \\
f_{(1;0)}\,f_{(1;1)} &= N\sqrt{\frac{2}{(N+1)(N+2)}}\,f_{(2;1)} + \sqrt{\frac{N-1}{N+1}}\,f_{(1;0)}\ , \\
f_{(0;1)}\,f_{(2;1)} &= N\sqrt{\frac{2}{(N+2)(N+3)}}\,f_{(2;2)} + N\sqrt{\frac{2}{(N+1)(N+2)}}\,f_{(1;1)} \quad .
\end{aligned}
\tag{A.8}
$$

Appendix B: Results for the Free Energy and the Mass Gap

We have computed the free energy to order 10 and the mass gap to order 4 in an θ-exact strong-coupling character expansion. The result for the free energy $\mathcal{F}$ is

$$
\begin{aligned}
&-\mathcal{F} = \frac{1}{V}\ln\mathcal{Z} = \\
&\quad 2\ln Z_0(\beta) + \ln[\frac{2}{\theta}\sin\frac{\theta}{2}] + {d_{(1;0)}}^2\left(\frac{\theta}{2\pi-\theta} - \frac{\theta}{2\pi+\theta}\right){z_{(1;0)}}^4 \\
&\quad +2{d_{(1;0)}}^2\left(\frac{\theta^2}{(2\pi-\theta)^2} + \frac{\theta^2}{(2\pi+\theta)^2}\right){z_{(1;0)}}^6
\end{aligned}
$$

$$
\begin{aligned}
&+{d_{(1;1)}}^2 {z_{(1;1)}}^4 + 5{d_{(1;0)}}^4 \frac{\theta^2}{(2\pi-\theta)\,(2\pi+\theta)} {z_{(1;0)}}^8 + \\
&{d_{(1;0)}}^2 \left(\frac{\theta^4}{(2\pi-\theta)^4} + \frac{\theta^4}{(2\pi+\theta)^4} \right) {z_{(1;0)}}^8 \\
&+6{d_{(1;0)}}^2 \left(\frac{\theta^3}{(2\pi-\theta)^3} - \frac{\theta^3}{(2\pi+\theta)^3} \right) {z_{(1;0)}}^8 \\
&-\frac{5}{2}{d_{(1;0)}}^4 \left(\frac{\theta^2}{(2\pi-\theta)^2} + \frac{\theta^2}{(2\pi+\theta)^2} \right) {z_{(1;0)}}^8 \\
&+2\sqrt{\frac{N-1}{N+1}} {d_{(1;0)}}^2 d_{(1;1)} \left(\frac{\theta^2}{(2\pi-\theta)^2} + \frac{\theta^2}{(2\pi+\theta)^2} \right) {z_{(1;0)}}^6 z_{(1;1)} \\
&-4\sqrt{\frac{2N}{N+1}} {d_{(1;0)}}^2 d_{(2;0)} \frac{\theta^2}{(2\pi-\theta)(2\pi+\theta)} {z_{(1;0)}}^6 z_{(2;0)} \\
&+{d_{(2;0)}}^2 \left(\frac{\theta}{\theta-4\pi} + \frac{\theta}{\theta+4\pi} \right) {z_{(2;0)}}^4 \\
&+2{d_{(1;0)}}^2 \left(\frac{\theta^6}{(2\pi-\theta)^6} + \frac{\theta^6}{(2\pi+\theta)^6} \right) {z_{(1;0)}}^{10} \\
&+8{d_{(1;0)}}^2 \left(\frac{\theta^5}{(2\pi-\theta)^5} - \frac{\theta^5}{(2\pi+\theta)^5} \right) {z_{(1;0)}}^{10} \\
&+18{d_{(1;0)}}^2 \left(\frac{\theta^4}{(2\pi-\theta)^4} + \frac{\theta^4}{(2\pi+\theta)^4} \right) {z_{(1;0)}}^{10} \\
&-16{d_{(1;0)}}^4 \left(\frac{\theta}{2\pi-\theta} - \frac{\theta}{2\pi+\theta} \right) \left(\frac{\theta^2}{(2\pi-\theta)^2} + \frac{\theta^2}{(2\pi+\theta)^2} \right) {z_{(1;0)}}^{10} \\
&+12\sqrt{\frac{N-1}{N+1}} {d_{(1;0)}}^2 d_{(1;1)} \left(\frac{\theta^3}{(2\pi-\theta)^3} - \frac{\theta^3}{(2\pi+\theta)^3} \right) {z_{(1;0)}}^8 z_{(1;1)} \\
&+4\sqrt{\frac{N-1}{N+1}} {d_{(1;0)}}^2 d_{(1;1)} \left(\frac{\theta}{2\pi-\theta} - \frac{\theta}{2\pi+\theta} \right) {z_{(1;0)}}^4 {z_{(1;1)}}^3 \\
&+12\sqrt{\frac{2N}{N+1}} {d_{(1;0)}}^2 d_{(2;0)} \left(\frac{\theta^3}{(2\pi-\theta)\,(2\pi+\theta)^2} - \frac{\theta^3}{(2\pi-\theta)^2\,(2\pi+\theta)} \right) {z_{(1;0)}}^8 z_{(2;0)} \\
&+4\sqrt{\frac{2N}{N+1}} {d_{(1;0)}}^2 d_{(2;0)} \left(\frac{\theta^2}{(2\pi-\theta)\,(\theta-4\pi)} - \frac{\theta^2}{(2\pi+\theta)\,(\theta+4\pi)} \right) {z_{(1;0)}}^4 {z_{(2;0)}}^3 \ .
\end{aligned}
\tag{B.1}
$$

For the mass gap up to order 4 in β, we obtained the result

$$
\begin{aligned}
&a \cdot m(\theta,\beta) = \\
&\quad -\ln z_{(1;1)} - 2\, z_{(1;1)} - 4\frac{N}{N+1} {z_{(1;0)}}^2 \left(\frac{\kappa\, a}{1-\kappa\, a} + \frac{\kappa\, b}{1-\kappa\, b} \right)
\end{aligned}
$$

$$
\begin{aligned}
&-\frac{N}{N+1}{z_{(1;0)}}^4\Bigg[9\left(\frac{\kappa\,a^2}{1-\kappa\,a^2}+\frac{\kappa\,b^2}{1-\kappa\,b^2}\right)+24\Bigg(\frac{a(\kappa\,a)^2}{(1-\kappa\,a)(1-\kappa\,a^2)}\\
&+\frac{b(\kappa\,b)^2}{(1-\kappa\,b)(1-\kappa\,b^2)}\Bigg)+16\left(\frac{a(\kappa\,a)^3}{(1-\kappa\,a^2)(1-\kappa\,a)^2}+\frac{b(\kappa\,b)^3}{(1-\kappa\,b^2)(1-\kappa\,b)^2}\right)\Bigg]\\
&+16\left(\frac{N}{N+1}\right)^2{z_{(1;0)}}^4\left(\frac{\kappa\,a}{1-\kappa\,a}+\frac{\kappa\,b}{1-\kappa\,b}\right)\left(\frac{\kappa\,a}{(1-\kappa\,a)^2}+\frac{\kappa\,b}{(1-\kappa\,b)^2}\right)\\
&+4\frac{N}{(N+1)^2}{z_{(1;0)}}^2 z_{(1;1)}\left[\frac{(\kappa\,a)^2}{(1-\kappa\,a)^2}+\frac{(\kappa\,b)^2}{(1-\kappa\,b)^2}\right]\\
&-8\left(\frac{N}{N+1}\right)^2{z_{(1;0)}}^2 z_{(2;0)}\,\frac{(\kappa\,a)(\kappa\,b)}{(1-\kappa\,a)(1-\kappa\,b)}\\
&+8\frac{N}{N+1}{z_{(1;0)}}^2 z_{(1;1)}\left[\frac{\kappa\,a}{(1-\kappa\,a)^2}+\frac{\kappa\,b}{(1-\kappa\,b)^2}\right]\\
&-2\,\frac{N^2}{N+1}{z_{(1;0)}}^3\,\frac{z_{(2;1)}}{z_{(1;1)}}\,(a+b)+2\,N{z_{(1;0)}}^4\,(a+b)\quad , \qquad \text{(B.2)}
\end{aligned}
$$

where

$$
\kappa=\frac{{z_{(1;0)}}^2}{z_{(1;1)}}\ ,\qquad a=\frac{\theta}{2\pi-\theta}\ ,\qquad \text{and}\qquad b=-\frac{\theta}{2\pi+\theta}\quad . \qquad \text{(B.3)}
$$

The above result is restricted to the β-dependent domain of

$$
|\theta|<2\pi\,\frac{z_{(1;1)}}{z_{(1;1)}+{z_{(1;0)}}^2}\approx 2\pi\,\frac{N}{2N+1}\,(1+O(\beta))\quad . \qquad \text{(B.4)}
$$

References

[1] A. Belavin, A. Polyakov,A. Schwartz and Y. Tyupkin, Phys. Lett. **59B** (1975) 85.

[2] C. Callan, R. Dashen and D. Gross, Phys. Lett. **63B** (1976) 334.

[3] R. Jackiw and C. Rebbi, Phys. Rev. Lett. **37** (1976) 172

[4] H. Fritzsch, M. Gell-Mann and H. Leutwyler, Phys. Lett. **47B** (1973) 365.

[5] S. Weinberg, Phys. Rev. **D11** (1975) 3583.

[6] G. 't Hooft, Phys. Rev. Lett. **37** (1976) 8.

[7] E. Witten, Nucl. Phys. **B156** (1979) 269.

[8] G. Veneziano, Nucl. Phys. **B59** (1979) 213.

[9] P. Woit, Phys. Rev. Lett. **51** (1983) 638.

[10] J. Hoek, M. Teper and J. Waterhouse, Phys. Lett. **180B** (1986) 112.

[11] M. Göckeler, A. S. Kronfeld, M. L. Laursen, G. Schierholz and U.-J. Wiese, Nucl. Phys. **B292** (1987) 349.

[12] M. Teper, Phys. Lett. **202B** (1988) 553.

[13] M. Campostrini, A. Di Gaicomo, H. Panagopoulos and E. Vicari, Nucl. Phys. **B329** (1990) 683.

[14] S. Adler, Phys. Rev. **177** (1969) 2426.

[15] J. Bell and R. Jackiw, Nuovo Cimento **60A** (1969) 47.

[16] V. Baluni, Phys. Rev. **D19** (1979) 2227.

[17] R. Crewther, P. Di Vecchia, G. Veneziano and E. Witten, Phys. Lett. **88B** (1979) 123.

[18] J. E. Kim, Phys. Rep. **150** (1987) 1.

[19] H. Y. Cheng, Phys. Rep. **158** (1988) 1.

[20] See Chapter 4 of R. N. Mohapatra, *Unification and Supersymmetry*, (Springer-Verlag New York, 1992) and references therein.

[21] R. Peccei and H. Quinn, Phys. Rev. Lett. **38** (1977) 1440.

[22] S. Weinberg, Phys. Rev. Lett. **40** (1978) 223.

[23] F. Wilczek, Phys. Rev. Lett. **40** (1978) 279.

[24] J.-E. Kim, Phys. Rev. Lett. **43** (1979) 103.

[25] A. R. Zhitnitsky, Sov. J. Nucl. Phys. **31** (1980) 260.

[26] M. Shifman, A. Vainshtein and V. Zakharov, Nucl. Phys. **B166** (1980) 493.

[27] M. Dine, W. Fischler and M. Srednicki, Phys. Lett. **104B** (1981) 199.

[28] M. Turner, Phys. Rep. **197** (1990) 1.

[29] H. Georgi and I. N. McArthur, Harvard University Report No. HUTP-81/A011, 1981 (unpublished).

[30] D. B. Kaplan and A. V. Manohar, Phys. Rev. Lett. **56** (1986) 2004.

[31] K. Choi, C. W Kim and W. K. Sze, Phys. Rev. Lett. **61** (1988) 794.

[32] S. Weinberg, Trans. N. Y. Acad. Sci. **38** (1977) 185.

[33] J. Gasser and H. Leutwyler, Phys. Rep. **87** (1982) 77.

[34] T. Banks, Y. Nir and N. Seiberg, in the proceedings of the 2nd IFT Workshop on Yukawa Couplings and the Origin of Mass, hep-ph/9403203.

[35] S. Samuel, Mod. Phys. Lett. **A7** (1992) 2007.

[36] A. D'Adda, M. Lüscher and P. Di Vecchia, Nucl. Phys. **B146** (1978) 63.

[37] E. Witten, Nucl. Phys. **B149** (1979) 285.

[38] S. Samuel, Phys. Rev. **D28** (1983) 2682.

[39] S. Olejnik and G. Schierholz, Nucl. Phys. B (Proc. Suppl.) **34** (1994) 709;
G. Schierholz, Nucl. Phys. B (Proc. Suppl.) **37A** (1994) 203.

[40] S. Coleman, Ann. Phys. **101** (1976) 239.

[41] N. Seiberg, Phys. Rev. Lett. **53** (1984) 637.

[42] G. Schierholz, Nucl. Phys. B (Proc. Suppl.) **42** (1995) 270.

[43] A. A. Migdal, JETP **42** (1976) 413.

[44] F. Green and S. Samuel, Nucl. Phys. **B194** (1982) 107.

[45] M. Stone, Nucl. Phys. **B152** (1979) 97.

[46] E. Rabinovici and S. Samuel, Phys. Lett. **101B** (1981) 323.

[47] K. G. Wilson, Phys. Rev. **D10** (1974) 2445.

[48] B. Berg and M. Lüscher, Nucl. Phys. **B190** (1981) 412.

[49] M. Lüscher Phys. Lett. **78B** (1978) 465.

[50] E. Witten, Phys. Lett. **86B** (1979) 283.

Figure Captions

Figure 1. A Lattice Link Configuration which Produces the Most General Plaquette-Variable Configuration for Open Boundary Conditions.

Figure 2a. The Free Energy Per Unit Volume $\mathcal{F}$ as a Function of θ. Shown here is the order-by-order case of CP^3 with $\beta = 0.6$.

Figure 2b. The Free Energy Per Unit Volume $\mathcal{F}$ as a Function of θ. Shown here is the case of CP^3 with $\beta = 0.7$.

Figure 3. The Phase Diagram for the CP^3 Model as Determined by the Tenth Order Free Energy Result.

Figure 4. The Fourth-Order Result for the Mass Gap am as a Function of β for Various Values of θ.

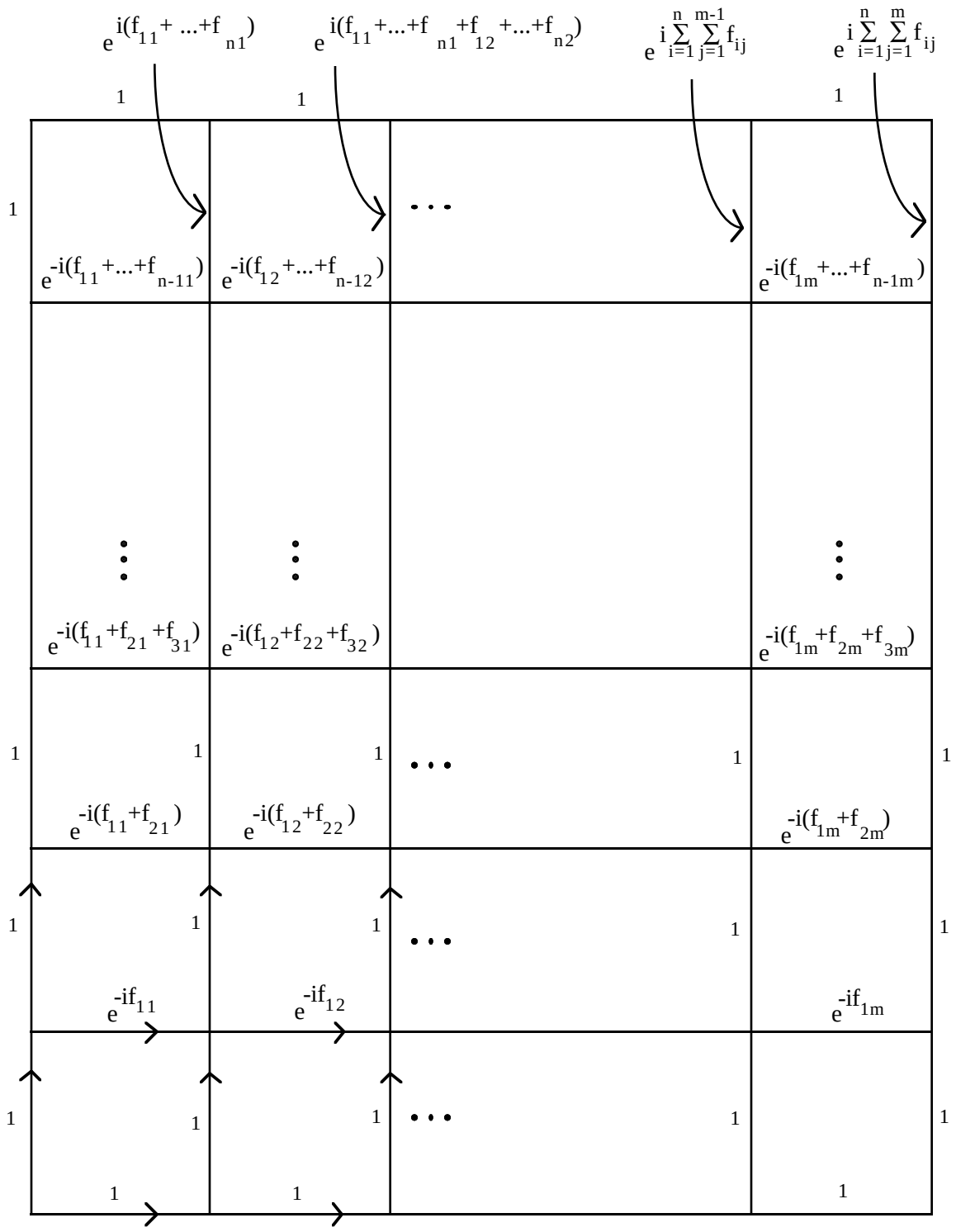
$e^{i(f_{11}+\ldots+f_{n1})}$
$e^{i(f_{11}+\ldots+f_{n1}+f_{12}+\ldots+f_{n2})}$
$e^{i\sum_{i=1}^{n}\sum_{j=1}^{m-1}f_{ij}}$
$e^{i\sum_{i=1}^{n}\sum_{j=1}^{m}f_{ij}}$
$e^{-i(f_{11}+\ldots+f_{n-11})}$
$e^{-i(f_{12}+\ldots+f_{n-12})}$
$e^{-i(f_{1m}+\ldots+f_{n-1m})}$
$e^{-i(f_{11}+f_{21}+f_{31})}$
$e^{-i(f_{12}+f_{22}+f_{32})}$
$e^{-i(f_{1m}+f_{2m}+f_{3m})}$
$e^{-i(f_{11}+f_{21})}$
$e^{-i(f_{12}+f_{22})}$
$e^{-i(f_{1m}+f_{2m})}$
$e^{-if_{11}}$
$e^{-if_{12}}$
$e^{-if_{1m}}$

Figure 1

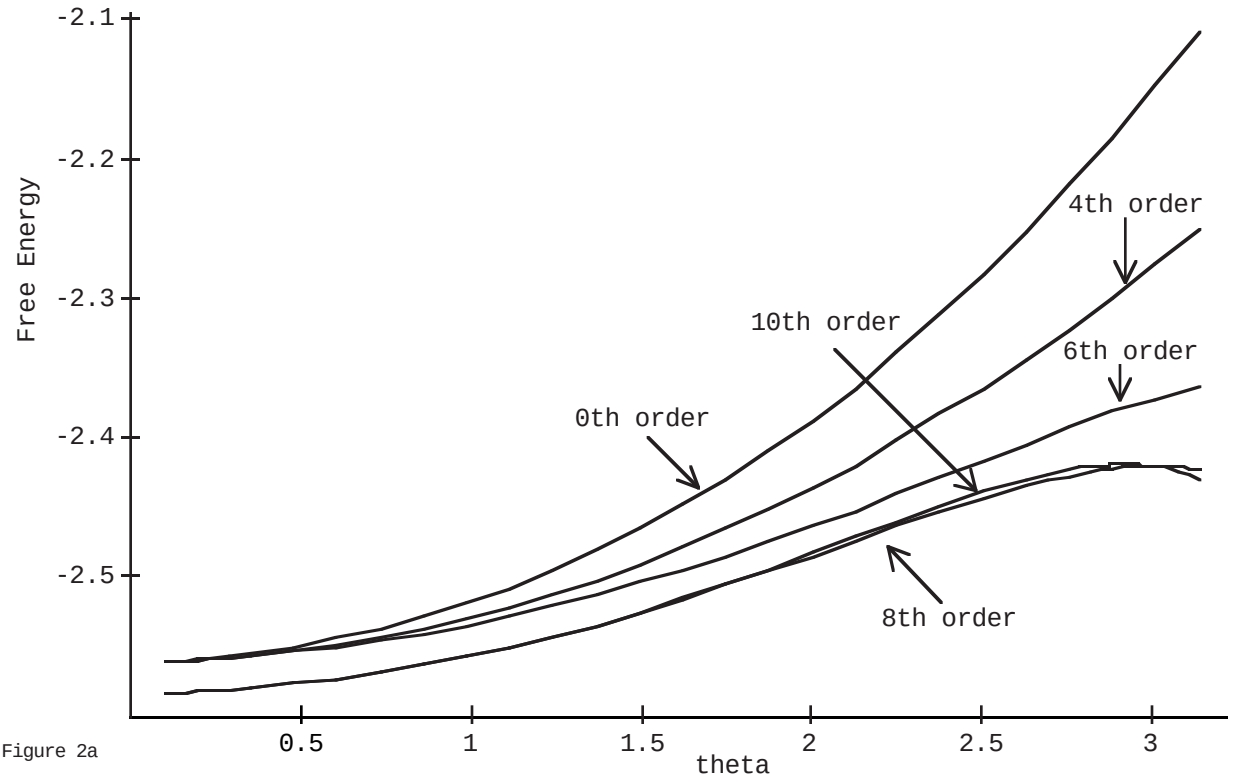

Figure 2a

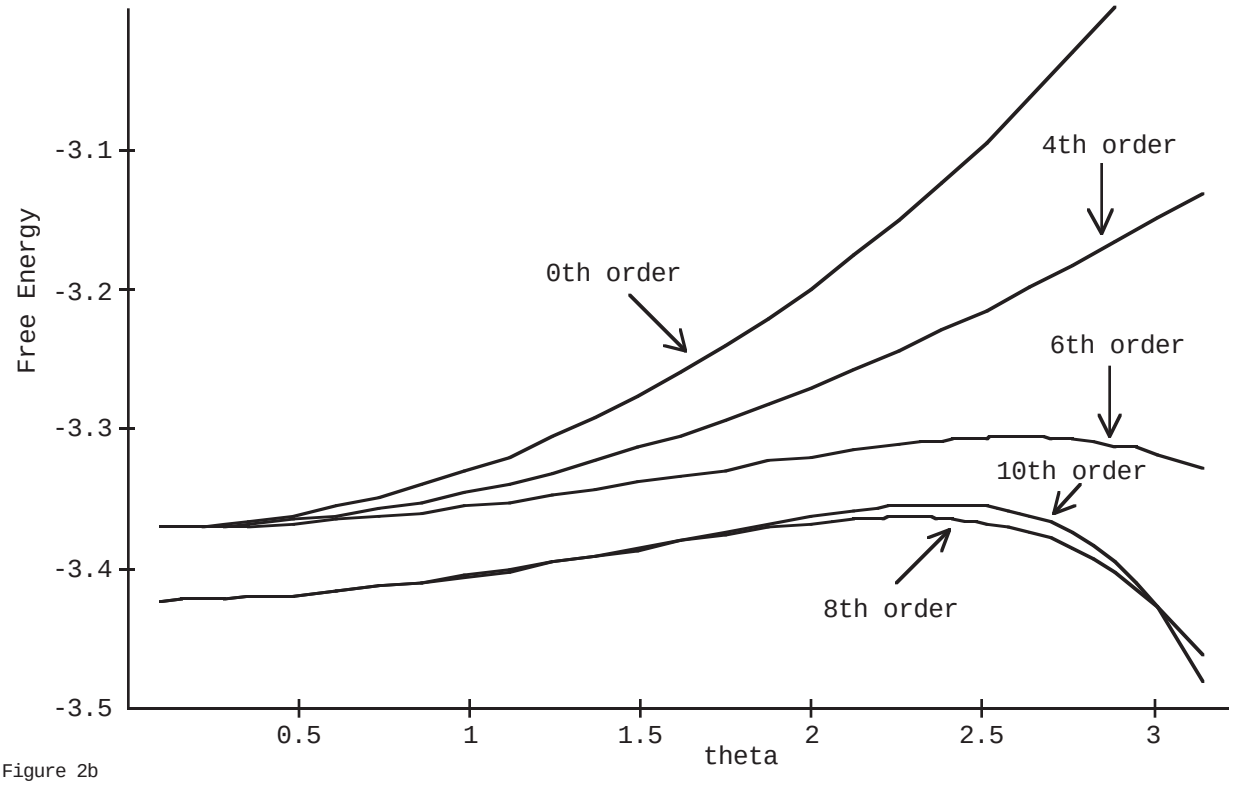

Figure 2b

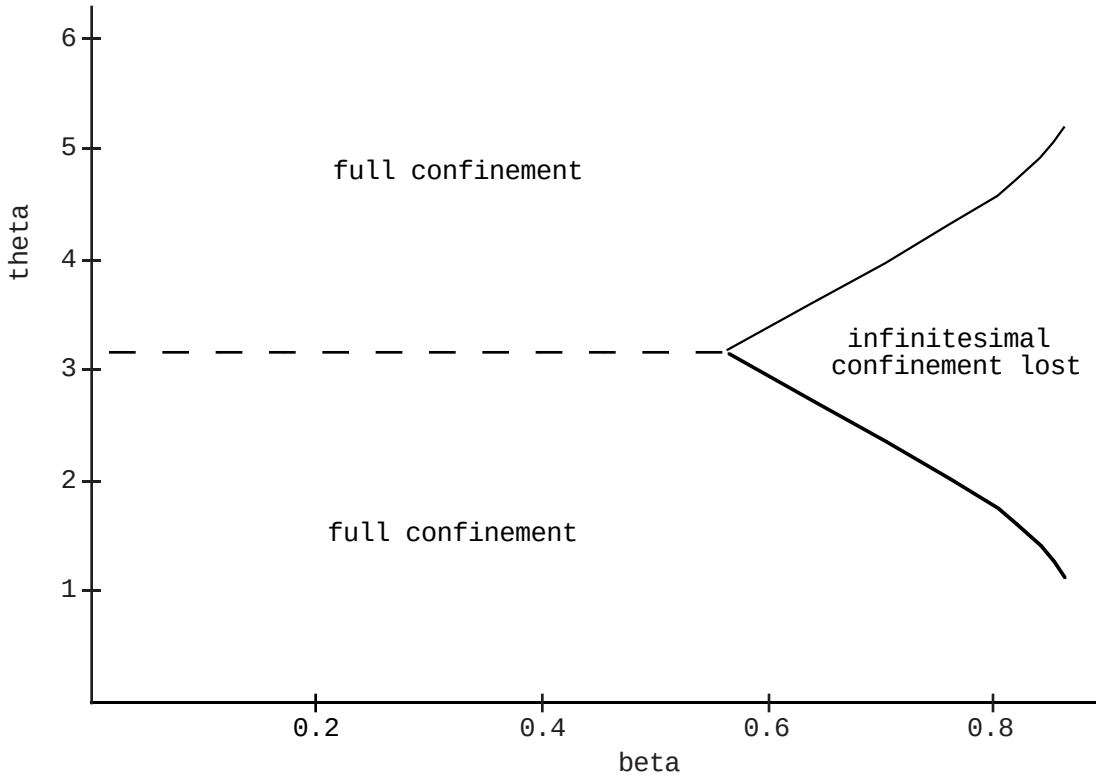
6
5
4
3
2
1
theta
full confinement
infinitesimal
confinement lost
full confinement
0.2
0.4
0.6
0.8
beta

figure 3

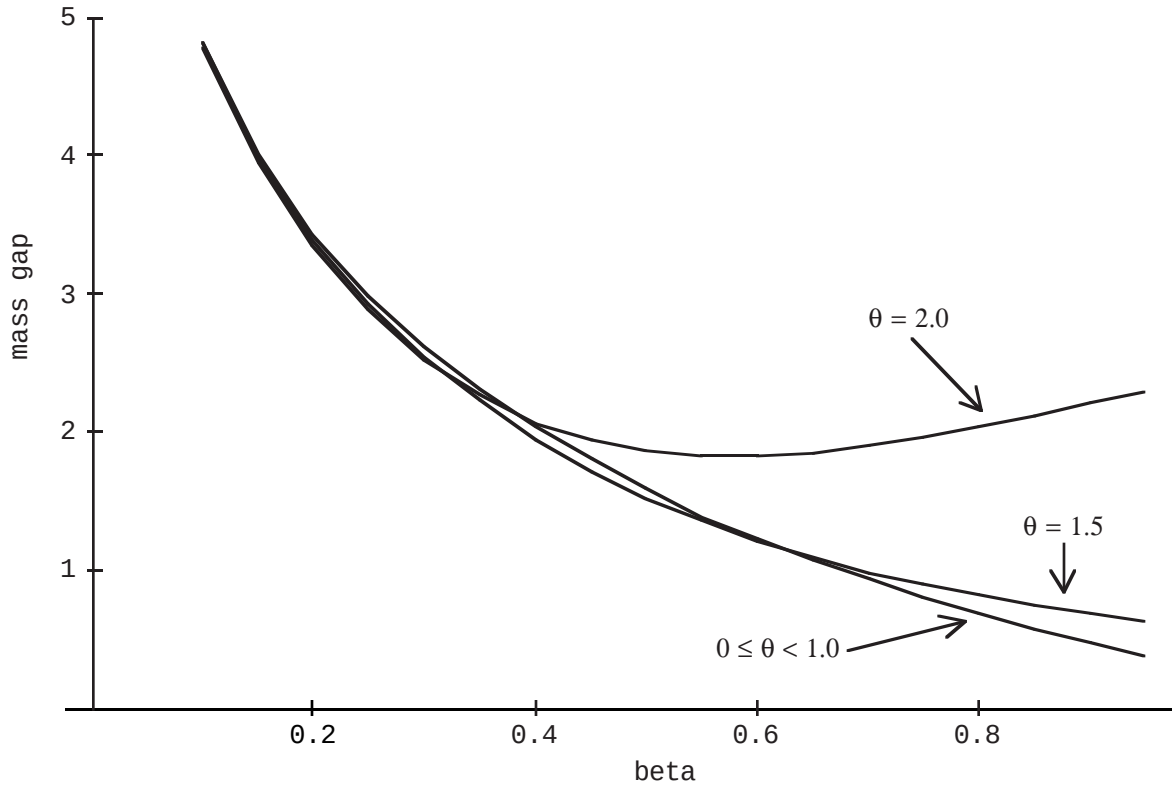

Figure 4